Proceedings of the Twenty-sixth (2016) International Ocean and Polar Engineering Conference **www.isope.org**
Rhodes, Greece, June 26-July 1, 2016

ISBN 978-1-880653-88-3; ISSN 1098-6189

Numerical Simulation of Effects of Two Different Baffles on Liquid Sloshing by MPS Method

Xiang Chen[1,2], Decheng Wan[1,2], Wenhua Huang[3]*

1 State Key Laboratory of Ocean Engineering, School of Naval Architecture, Ocean and Civil Engineering, Shanghai Jiao Tong University,
2 Collaborative Innovation Center for Advanced Ship and Deep-Sea Exploration, Shanghai, China
3 School of Science, Huzhou University, Huzhou, China
*Corresponding author

ABSTRACT

In this paper, a series of numerical models has been developed to study the effects of two different baffles on liquid sloshing under the six degree-of-freedom (6-DOF) excitation. The moving particle semi-implicit (MPS) method is a mesh-free method which can simulate flow with large deformation and nonlinear fragmentation of free surface effectively. The MLParticle-SJTU solver based on improved MPS method is first validated against the available experimental data for 3-D liquid sloshing in a rectangular tank under horizontal excitation. Then, the study of liquid sloshing in another tank is carried out under the 6-DOF excitation. The detailed flow field and the variation of impact pressure can be observed clearly. In addition, the effects of two different baffle types on liquid sloshing, two vertical baffle and two ring baffles, are further analyzed based on previous rectangular tank. Results show that the sloshing and pressure amplitudes are obviously reduced due to these baffles and the ring baffles are more effective on restraining sloshing.

KEY WORDS: Liquid sloshing; baffles; MPS; 6-DOF excitation.

INTRODUCTION

With the development of shipping industry, a mass of large vessels which load liquid specially has been constructed such as VLCC, LNGC, LPGC and so on. Because of the increase of frequency and intensity of sea condition, the navigation safety of liquid cargo vessels has been the focus of research. When external excitations are large amplitude or near resonant frequency, the liquid inside a partially filled tank will be prone to complicated and nonlinear sloshing phenomenon. The impact pressure induced by liquid sloshing may destroy the structure of tank walls and even cause more violent ship rolling. So, designing a liquid cargo rationally and predicting its motion accurately are significant for the transportation of liquid cargo.

Rising interest in liquid sloshing, many studies of theory, experiment and numerical simulation have been conducted. At the outset, original researchers had to study 2D liquid sloshing by the limit of relevant knowledge and computational capabilities. Faltinsen (1978) developed a linear analytical solution for liquid sloshing in 2-D rectangular tank under horizontal excitation. Then this solution has been widely employed in a mass of numerical models. Nakayama and Washizu (1980) simulated non-linear liquid sloshing in a 2-D rectangular tank under pitch excitation by using the finite element method (FEM). Subsequently, Nakayama and Washizu (1981) also used the boundary element method (BEM) to analyze the 2-D problem of non-linear liquid sloshing. Cho and Lee (2004) simulated numerically a 2-D tank to study the large amplitude liquid sloshing. Wang and Khoo (2005) studied the 2-D liquid sloshing under random excitations by the fully non-linear wave theory. Frandsen et al. (2003, 2004) conducted a series of numerical simulations of liquid sloshing in 2-D tank under horizontal and vertical excitations in σ-coordinate. Chen et al. (2004, 2005) used Navier–Stokes equations (NSE) to study 2-D viscous liquid sloshing under 3-DOF (surge, heave and pitch) excitation. Shao et al. (2012) applied another mesh-free method, smoothed particle hydrodynamics (SPH), to model 2-D liquid sloshing dynamics. Yang et al. (2015) investigated the effects of external excitation period on 2-D liquid sloshing based on MPS.

With the development of research, the problem of 3-D liquid sloshing has been analyzed. Wu et al. (1998) simulated a 3-D tank for studying liquid sloshing by using FEM. In addition, Koh et al. (1998) developed a coupled BEM-FEM for analyzing 3-D liquid sloshing in rectangular tanks. Kim (2001) simulated the sloshing flow in 2-D and 3-D containers by using a finite difference method. Kim et al. (2004) studied numerically slosh-induced impact pressures in 3-D and 2-D prismatic tanks, respectively. Liu and Lin (2008) simulated a 3-D two-phase flow model to study non-linear liquid sloshing under 6-DOF excitation. Then, Liu and Lin (2009) further studied liquid sloshing in a 3-D tank with a horizontal baffle and a vertical baffle under multiple DOF, respectively. Wu and Chen (2009) used a time-independent finite difference method to research sloshing waves and resonance modes of fluid in a 3-D tank. Xue and Lin (2011) conducted a 3-D numerical study of ring baffle effects on reducing violent liquid sloshing by virtual boundary force (VBF) method. Lee et al. (2011) made a

numerical simulation of 3-D sloshing based on a finite difference method. Koh et al. (2013) used the improved consistent particle method (CPM) to simulate liquid sloshing with constrained floating baffle in 3-D prismatic tanks.

In this study, the MLParticle-SJTU solver based on improved MPS method is employed for numerical simulation of 3-D liquid sloshing. In first section, a short description of MPS method follows. In second section, a rectangular tank without baffles (Tank A) is modeled under horizontal excitation. In addition, the liquid sloshing under angular excitation is simulated in former research. The MLParticle-SJTU solver is valid for the simulation of sloshing under 6-DOF excitation by comparing numerical results with experimental data. The impact pressures on tank walls are in a good agreement with experimental data. And the MLParticle-SJTU solver can simulate the complex flow phenomena such as breaking wave, splashing and so on. In a real marine environment, the external excitation of the tank involves multiple DOF. So next we simulate liquid sloshing in another tank without baffles (Tank B) under 6-DOF excitation. The impact pressure and the deformation of free surface can be observed clearly in the animation of the computational results. Finally, the effects of two different baffles on liquid sloshing under 6-DOF excitation are investigated. In case 1, two vertical baffles are installed on the bottom. And two ring baffles are placed around the walls in case 2. The numerical results, including the impact pressure and flow field, are compared to the previous case without baffles.

MOVING PARTICLE SEMI-IMPLICIT (MPS) METHOD

Koshizuka and Oka (1996) have explained the MPS method in detail. The afterward researchers (Tanaka and Masunaga, 2010; Lee et al., 2011; Zhang and Wan, 2014) further modified MPS method for improving numerical accuracy. The MPS method contains several following numerical models.

Governing Equations

For incompressible and viscous fluid, governing equations include mass and momentum conservation equations. They can be presented as:

$$\frac{1}{\rho}\frac{D\rho}{Dt} = \nabla \cdot \vec{V} = 0 \tag{1}$$

$$\frac{D\vec{V}}{Dt} = -\frac{1}{\rho}\nabla P + \nu\nabla^2\vec{V} + \vec{g} \tag{2}$$

where ρ is the fluid density, t is the time, $\vec{V}$ is the velocity vector, P is the pressure, ν is the kinematic viscosity and $\vec{g}$ is the gravitational acceleration vector.

Particle Interaction Models

Kernel Function

In MPS method, governing equations are transformed to particle interaction equations. The interaction between particles is described through a kernel function. The kernel function adopted in this paper is as follows:

$$W(r) = \begin{cases} \dfrac{r_e}{0.85r + 0.15r_e} - 1 & 0 \le r < r_e \\ 0 & r_e \le r \end{cases} \tag{3}$$

where r is the distance between two particles and r_e is the radius of the particle interaction. The particle number density and gradient model is r_e=2.1l_0, while r_e=4.0l_0 is used for the Laplacian model, where l_0 is the initial distance between two adjacent particles.

Gradient Model

In this paper, the gradient operator is modeled as a local weighted average of the gradient vectors between particle i and its neighboring particle j, it can be written as:

$$<\nabla P>_i = \frac{D}{n^0}\sum_{j\neq i}\frac{P_j + P_i}{|\vec{r}_j - \vec{r}_i|^2}(\vec{r}_j - \vec{r}_i)\cdot W(|\vec{r}_j - \vec{r}_i|) \tag{4}$$

where D is the number of space dimension, n^0 is the initial particle number density and $\vec{r}$ is coordinate vector of fluid particle.

Laplacian Model

The Laplacian operator is modeled by weighted average of the distribution of a quantity ϕ from particle i to its neighboring particle j, it can be described as:

$$<\nabla^2\phi>_i = \frac{2D}{n^0\lambda}\sum_{j\neq i}(\phi_j - \phi_i)\cdot W(|\vec{r}_j - \vec{r}_i|) \tag{5}$$

$$\lambda = \frac{\sum_{j\neq i} W(|\vec{r}_j - \vec{r}_i|)\cdot|\vec{r}_j - \vec{r}_i|^2}{\sum_{j\neq i} W(|\vec{r}_j - \vec{r}_i|)} \tag{6}$$

where λ is applied to make sure that the increase of variance is equal to the analytical solution.

Model of Incompressibility

Tanaka et al. (2010) proposed a mixed source term method, which combines velocity divergence and particle number density. And Lee et al. (2011) rewrote the Poisson equation of pressure (PPE) as:

$$<\nabla^2 P^{k+1}>_i = (1-\gamma)\frac{\rho}{\Delta t}\nabla\cdot\vec{V}_i^* - \gamma\frac{\rho}{\Delta t^2}\frac{<n^*>_i - n^0}{n^0} \tag{7}$$

where γ is a blending parameter which varies from 0 to 1, n^* is the temporal particle number density and Δt is the time step. In this paper, γ=0.01 is employed for all numerical simulations.

Free Surface Detection

A modified surface particle detection method (Zhang, 2012a) which is based on the asymmetry arrangement of neighboring particles shown in Fig. 1 is employed in this paper. And it can read as the following equations:

$$<\vec{F}>_i = \frac{D}{n^0}\sum_{j\neq i}\frac{1}{|\vec{r}_i - \vec{r}_j|}(\vec{r}_i - \vec{r}_j)W(r_{ij}) \tag{8}$$

$$<|\vec{F}|>_i \; > \alpha \tag{9}$$

$$\alpha = 0.9\left|\vec{F}\right|^0 \tag{10}$$

where $\vec{F}$ is a vector which represents the asymmetry of arrangements of neighbor particles, $\left|\vec{F}\right|^0$ is the initial value of $\left|\vec{F}\right|$.

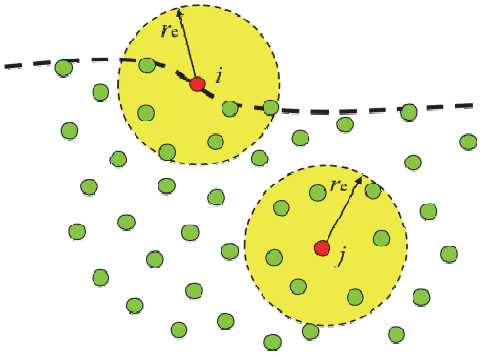

Fig. 1 A schematic view of particle interaction domain

NUMERICAL SIMULATIONS

In this section, the focus of our work is to study the effects of two different baffles on liquid sloshing under 6-DOF excitation by using MLParticle-SJTU solver based on improved MPS method. In order to confirm the validity of MLParticle-SJTU solver, a 3-D rectangular tank (Tank A) is modeled to simulate liquid sloshing under horizontal excitation according to the experimental research of others. It is essential to note that, 3-D liquid sloshing under angular excitation has been investigated in earlier studies by other members of our group (Yang et al., 2015). By comparing numerical results and experimental data, MLParticle-SJTU solver is valid to simulate liquid sloshing under horizontal excitation. Then another rectangular tank (Tank B), a common liquid storage for research and application, is chosen to simulate 3-D liquid sloshing under 6-DOF excitation. Two different kinds of baffles are further modeled to study their effects on liquid sloshing.

Model validation

In this section, 3-D liquid sloshing in Tank A under horizontal excitation is simulated to validate MLParticle-SJTU solver, which is the same as the experimental model given by Kang and Lee (2005). The geometry of the liquid sloshing system is shown in Fig. 2, and its dimensions are 0.8m (L_A), 0.35m (B_A), 0.5m (H_A) and 0.15m (D_A). The external excitation applied on the tank is:

$$X = A \cdot \sin(\omega \cdot t) \tag{11}$$

where A is the amplitude of excitation which is set to 0.02 m and ω is the excitation frequency with the value of 4.967 rad/s. In this case, total 542376 particles are used to simulate this model. The initial particle space is 0.005 m, the time step is 5×10^{-4} s and the density of liquid is 1000 kg/m^3. Two pressure probes are placed to measure the variation of pressure. Table 1 presents the arrangement of pressure probes and Fig. 4 shows the variation of probe pressure compared to the data of experiment. In addition, some snapshots of experiment and numerical simulation are shown in Figs. 3(a)~(h).

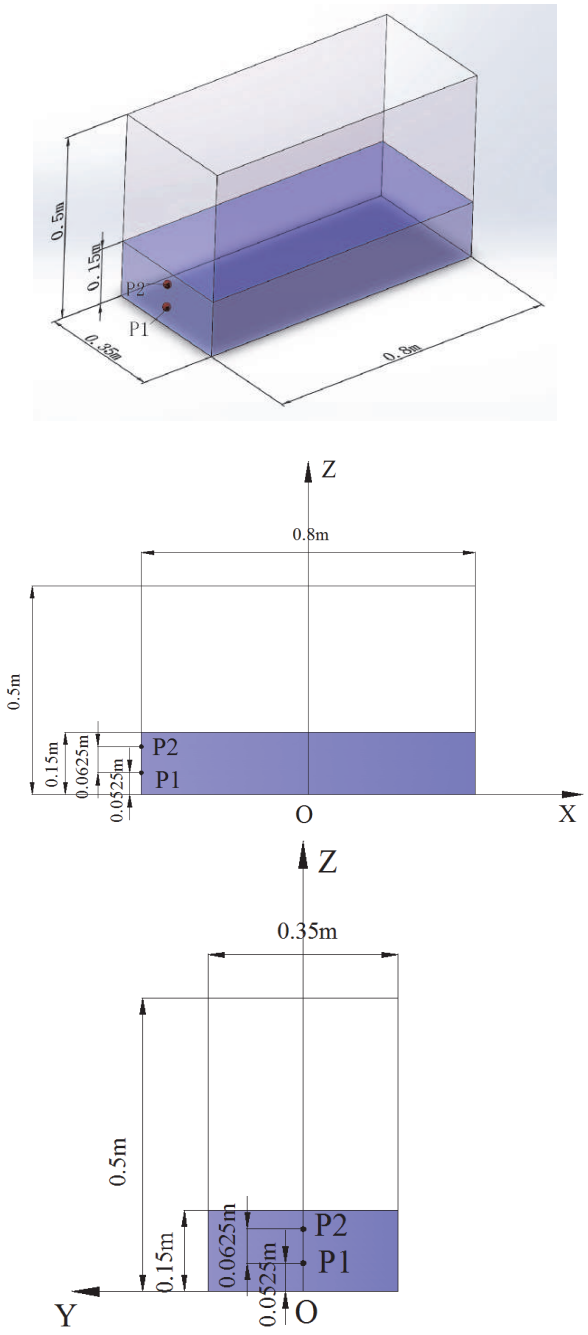

Fig. 2 The sketch of Tank A

Table 1 The arrangement of pressure probes in Tank A

	X [m]	Y [m]	Z [m]
P1	-0.4	0	0.0525
P2	-0.4	0	0.115

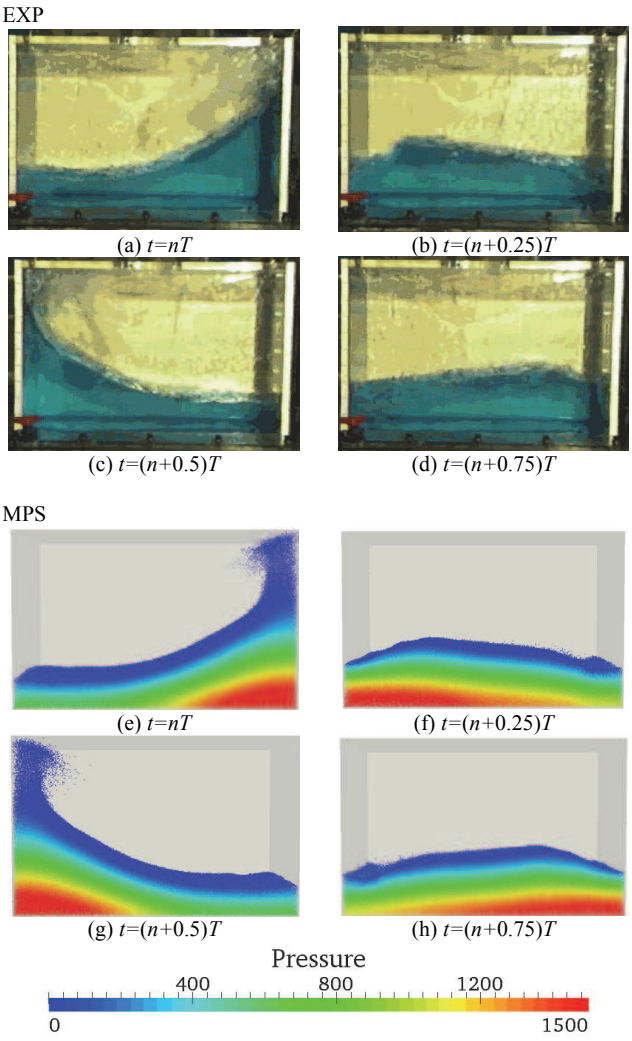

Fig. 3 Comparison of the flow patterns between experiment and numerical simulation.

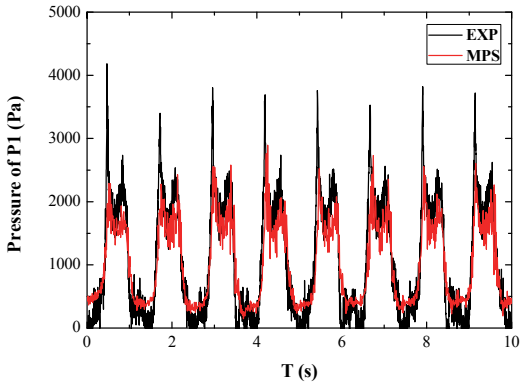

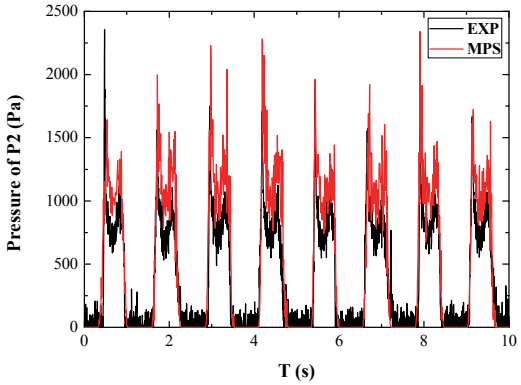

Fig. 4 Comparison of pressures on P1 and P2 among experimental and numerical results

From Fig. 3, the nonlinear deformation and large fragmentation of free surface can be observed. The numerical simulation of flow field is in good agreement with the experiment. And many details about flow field such as breaking wave and local splashing are clearly captured. The fluid runs up along the side wall, impacts the ceiling of the tank and drops down under the action of gravity. The numerical results show a good congruency with pressures on P1 and P2 of experiment in Fig. 4. Two successive pressure peaks in each period may be noticed, which explains the phase difference between tank motion and liquid motion. When the tank reaches to the maximum horizontal displacement and move to the opposite direction, the later water that reaches to the side wall results in the first high impact pressure. The second pressure peak results from the water that runs up to the highest point and drops down to the free surface.

Tank B without baffles

In view of real marine environment, the tank is excited in multiple DOF. In this section, the liquid sloshing in another rectangular tank under 6-DOF excitation is simulated. The sketch of Tank B is shown in Fig. 5. Tank B is 0.8 m long (L_B), 0.8 m wide (W_B) , 0.54 m high (H_B) and the depth of still water is 0.368m (D_B). In this simulation, 883264 particles are used, the initial particle space is 0.007 m and the time step is 5×10^{-4} s. The density of water is also 1000 kg/m^3. Under external excitation, Tank B moves according to:

$$X = A \cdot \sin(\omega \cdot t + \varphi) \tag{12}$$

where X is the horizontal or angular displacement, A is the amplitude, ω is excited frequency and φ is initial phase. The excited frequency is set to 5.818 rad/s for every DOF. Moreover, the center of rotation is the geometric center of Tank B. The amplitude and initial phase of every DOF are listed in Table 2.

Table 2 The amplitude and initial phase of every DOF

	Surge	Sway	Heave	Pitch	Roll	Yaw
Amplitude	0.01m	0.01m	0.005m	4°	4°	2°
Initial Phase	0°	90°	0°	90°	0°	0°

The variation of pressure on the walls is measured by two pressure probes. The positions of pressure probes are listed in Table 3. And the time history of pressure is presented in Fig. 7.

Table 3 The arrangement of pressure probes in Tank B

	X [m]	Y [m]	Z [m]
P1	-0.4	0.2	0.135
P2	-0.4	-0.2	0.135

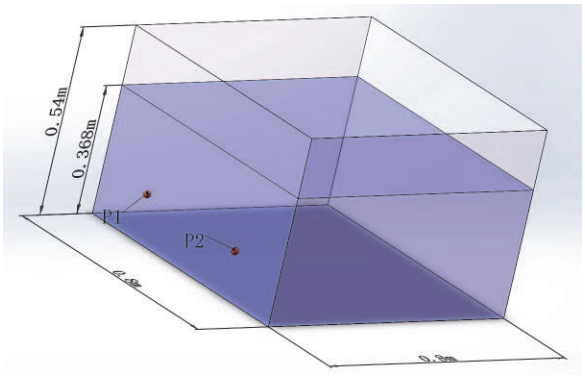

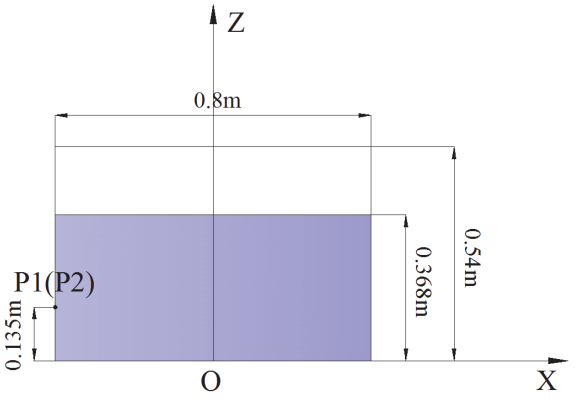

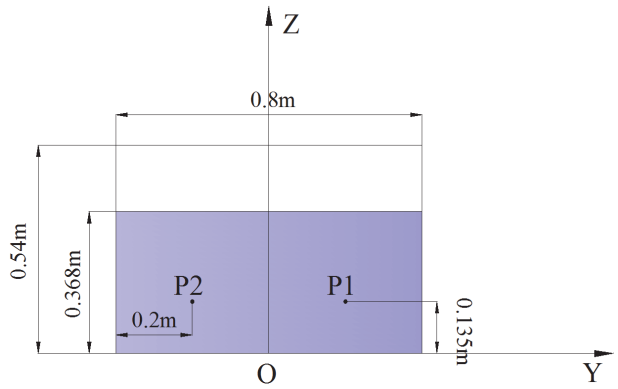

Fig. 5 The sketch of Tank B without baffles

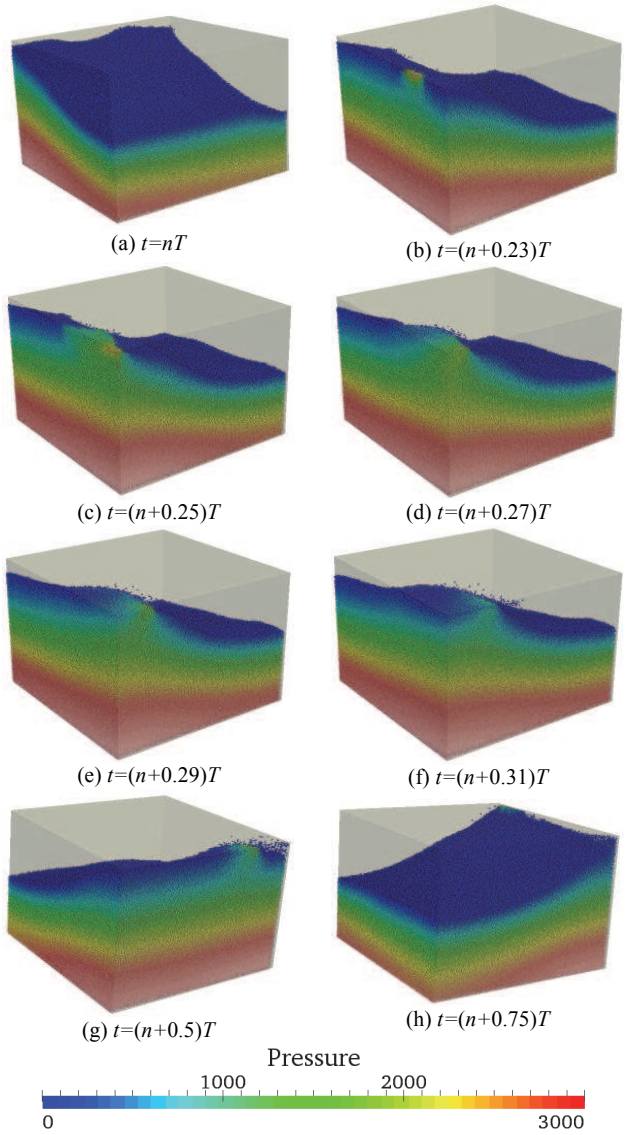

Fig. 6 Snapshots of pressure field in Tank B without baffles

The snapshots of different time instants are illustrated in Figs. 6(a)~(h). The phenomena of liquid sloshing under 6-DOF excitation are complex. Although the amplitude of every DOF is small, the sloshing is still so violent that water hits the ceiling of the tank. Comparing the details among Figs. 6(b)~(f), pressure peaks appear in multi places within a short time, not only at the corner of ceiling. At the time of first pressure peak, the motions of water and tank are opposite which generates local slamming. When the corner of ceiling is at its low point, the second pressure peak appears. And the third pressure peak of the ceiling results from the inertia of water.

Fig. 7 shows the variation of pressure at two probes, P1 and P2. It is seen that with the movement of the tank, the measured pressure values rise and fall periodically. Comparing the pressures of P1 and P2, the extent of variation of pressure is smaller for P2. The final direction

of movement of tank B is anticlockwise, combining the motions of every DOF. So, the pressure peak of P1 is earlier to appear than that of P2 in the same period.

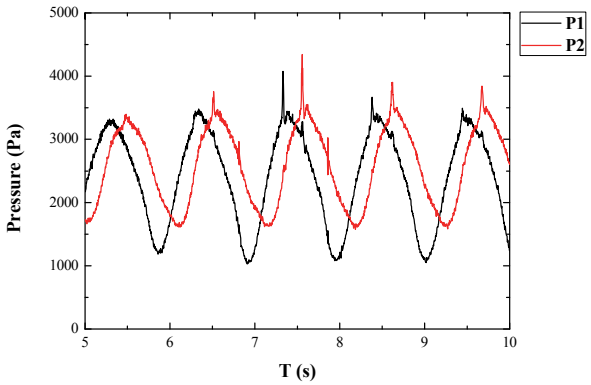

Fig. 7 The time history of pressure for Tank B

Tank B with two different baffles

In this section, two computational models are similar to the model in the previous section, but two different kinds of baffles are placed in Tank B. In case 1, two vertical baffles of the same dimensions are mounted on the bottom of tank. And the surrounding walls of Tank B are installed by two ring baffles in case 2. The detailed illustration of two models are presented in Figs. 8~9. In these models, the initial particle space is changed to 0.007 m, so 883260 and 891534 particles are used for case 1 and case 2. The parameters of external excitation and the arrangement of two pressure probes are as same as previous section. Figs. 10(a)~(h) show some snapshots of two models at different time instants, respectively. And the variations of pressures with time are depicted in Figs. 11~12.

The deformation of free surface from Fig. 10 shows that the sloshing amplitude are reduced obviously, comparing to Fig. 6. Observing Figs. 10(a)~(d) carefully, we can discover that only a spot of liquid hits the ceiling of the tank and the intensity of slamming has been reduced. Making a comparison to no baffles, the nonlinear fragmentation of free surface such as breaking wave and local splashing are undetectable in case 1. The phenomena of multi pressure peaks in a short time disappears. From Figs. 10(e)~(g), the whole flow field are divided into four subfields by the arrangement of two ring baffles in case 2. For each subfield, the mass of liquid available for sloshing is reduced. Near ring baffles, the drop of adjacent free surface can be observed. And the water climbs along the ring baffles. The disappearance of local slamming and impact pressure on the top wall occurs at the same time. The sloshing amplitude is much smaller than previous two models.

Comparing Fig. 7 and Figs. 11~12, the values of pressure are reduced greatly by the effect of baffles. For P1 and P2, the pressure peaks of no baffles are the largest and the pressure peaks of ring baffles are the smallest. The ring baffles (case 2) are more effective on reducing impact pressure. Furthermore, the pressure valley of case 2 is the largest by making a comparison among the minimum values of every pressure probe for each case. These results reveal that the wave height of free surface varies very little in case 2. The phase lag of pressure in case 1 and 2 are obvious by making a comparison to the pressure of no baffles. This is attributed to the damping effect of baffles.

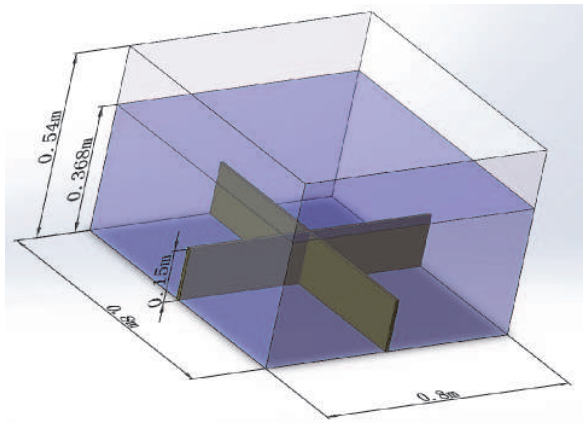

Fig. 8 The 3-D sketch of Case 1

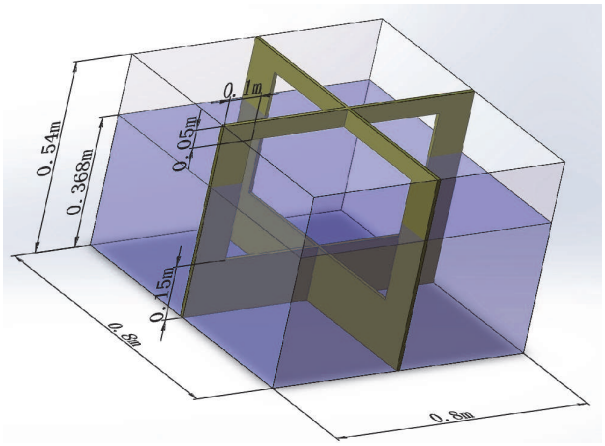

Fig. 9 The 3-D sketch of Case 2

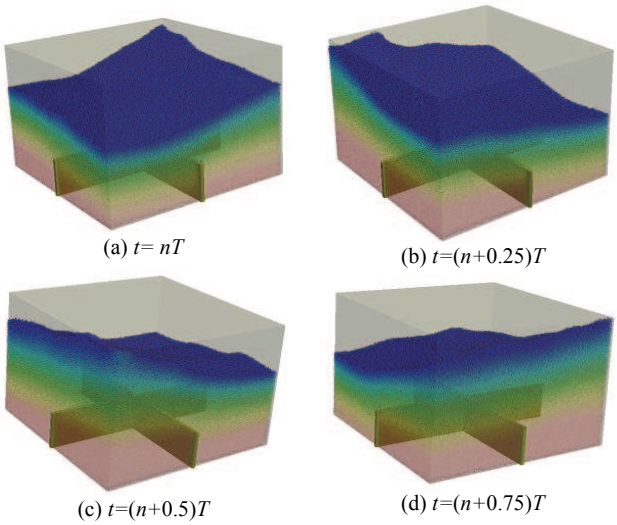

(a) $t= nT$ (b) $t=(n+0.25)T$

(c) $t=(n+0.5)T$ (d) $t=(n+0.75)T$

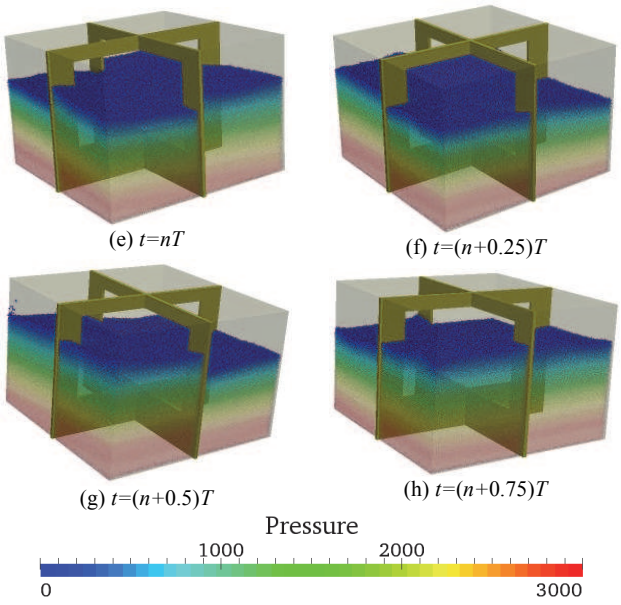

Fig. 10 Snapshots of pressure field in Tank B with two different baffles

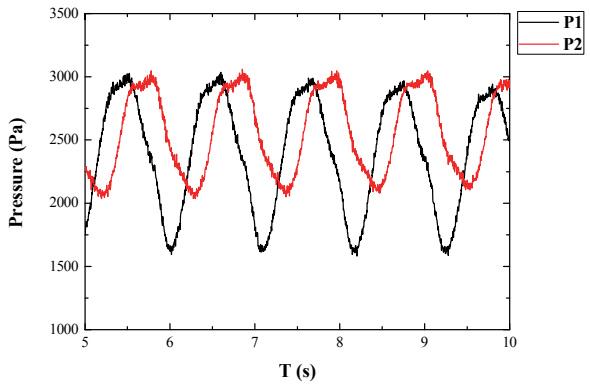

Fig. 11 The time history of pressure for case 1

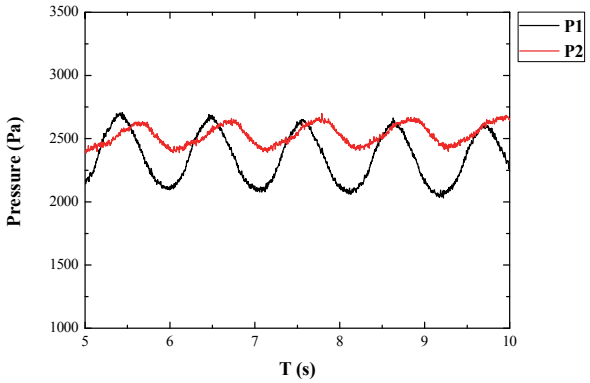

Fig. 12 The time history of pressure for case 2

CONCLUSIONS

In this paper, the effects of two different baffles on 3-D liquid sloshing under 6-DOF excitation are investigated by MLParticle-SJTU solver based on improved MPS method. A series of numerical simulations is carried out. Based on the results, the following conclusions can be drawn:

(1) The impact pressure of numerical simulation on the measuring probes in a 3-D tank (Tank A) under horizontal excitation shows a good agreement with the experimental data, which illustrates that MLParticle-SJTU solver is valid. And the validity of MLParticle-SJTU solver for angular excitation is confirmed in former research. The large deformation and nonlinear fragmentation of free surface, like breaking wave, splashing, hitting the roof and so on, are observed clearly in this simulation. And the typical two successive pressure peaks in each period can be noticed.

(2) The variation of pressure and the deformation of free surface are captured well in another tank (Tank B) without baffles under 6-DOF excitation. Some complex flow phenomena such as hitting the ceiling of tank many times in a short time and splashing are observed.

(3) Based on Tank B, two kinds of baffles are arranged. The first baffles are two vertical baffles, mounted on the bottom of tank. In another case, two ring baffles are installed around surrounding walls. All kinds of baffles are effective on reducing the intensity of sloshing and the pressure amplitude. Furthermore, ring baffles has better effect on restraining sloshing by dividing the fluid into four subfields and reducing the mass of liquid available for sloshing.

ACKNOWLEDGEMENTS

This work is supported by the National Natural Science Foundation of China (51379125, 51490675, 11432009, 51579145, 11272120), Chang Jiang Scholars Program (T2014099), Program for Professor of Special Appointment (Eastern Scholar) at Shanghai Institutions of Higher Learning (2013022), Innovative Special Project of Numerical Tank of Ministry of Industry and Information Technology of China (2016-23) and Foundation of State Ley Laboratory of Ocean Engineering (GKZD010065), to which the authors are most grateful.

REFERENCES

Chen, BF (2005). "Viscous fluid in a tank under coupled surge, heave and pitch motions," *Journal of Waterway Port Coastal and Ocean Engineering*, 131 (5), 239-256.

Chen, BF, Nokes, R (2005). "Time-independent finite difference analysis of 2D and nonlinear viscous liquid sloshing in a rectangular tank," *Journal of Computational Physics*, 209 (1), 47-81.

Cho, JR, Lee, HW (2004). "Non-linear finite element analysis of large amplitude sloshing flow in two-dimensional tank," *International Journal for Numerical Methods in Engineering*, 61 (4), 514-531.

Frandsen, JB, Borthwick, AGL (2003). "Simulation of sloshing motions in fixed and vertically excited containers using a 2-D inviscid σ-transformed finite difference solver," *Journal of Fluids and Structures*, 18 (2), 197-214.

Frandsen, JB (2004). "Sloshing motions in excited tanks," *Journal of Computational Physics*, 196 (1), 53-87.

Faltinsen, OM (1978). "A Numerical Nonlinear Method of Sloshing in

Tanks with Two Dimensional Flow," *Journal of Ship Research*, 22 (3), 193–202.

Kang, DH, Lee, YB (2005). "Summary Report of Sloshing Model Test for Rectangular Model," Daewoo Ship building & Marine Engineering Co., Ltd. (DSME), South Korea.

Kim, Y (2001). "Numerical simulation of sloshing flow with impact load," *Applied Ocean Research*, 23, 53-62.

Kim, Y, Shin, YS, Lee, KH (2004). "Numerical study on slosh-induced impact pressures," *Applied Ocean Research*, 26, 213-226.

Koh, CG, Luo, M, Gao, M, Bai, W (2013). "Modeling of liquid sloshing with constrained floating baffle," *Computers and Structures*, 122, 270-279.

Koh, HM, Kim, JK, Park, JH (1998). "Fluid-structure interaction analysis of 3-D rectangular tanks by a variationally coupled BEM–FEM and comparison with test results," *Earthquake Engineering and Structural Dynamics*, 27 (27), 109-124.

Koshizuka, S, Oka, Y (1996). "Moving-particle semi-implicit method for fragmentation of incompressible fluid," *Nuclear Science and Engineering*, 123 (3), 421–434.

Lee, BH, Park, JC, Kim, MH, Hwang, SC, (2011). "Step-by-step improvement of MPS method in simulating violent free-surface motions and impact-loads," *Computer Methods in Applied Mechanics and Engineering*, 200 (9-12), 1113-1125.

Lee, SH, Lee, YG, Jeong, KL (2011). "Numerical simulation of three-dimensional sloshing phenomena using a finite difference method with marker-density scheme," *Ocean Engineering*, 38, 206-225.

Liu, DM, Lin, PZ (2008). "A numerical study of three-dimensional liquid sloshing in tanks," *Journal of Computational Physics*, 227, 3921-3939.

Liu, DM, Lin, PZ (2009). "Three-dimensional liquid sloshing in a tank with baffles," *Ocean Engineering*, 36, 202-212.

Nakayama, T, Washizu, K (1980). "Nonlinear analysis of liquid motion in a container subjected to forced pitching oscillation," *International Journal for Numerical Methods in Engineering*, 15 (8), 1207-1220.

Nakayama, T, Washizu, K (1981). "The boundary element method applied to the analysis of two-dimensional nonlinear sloshing problems," *International Journal for Numerical Methods in Engineering*, 17 (11), 1631-1646.

Shao, JR, Li, HQ, Liu, GR, Liu, MB (2012). "An improved SPH method for modeling liquid sloshing dynamics," *Computers and Structures*, 100-101, 18-26.

Tanaka, M, Masunaga, T, (2010). "Stabilization and smoothing of pressure in MPS method by Quasi-Compressibility," *Journal of Computational Physics*, 229 (11), 4279-4290.

Wang, CZ, Khoo, BC (2005). "Finite element analysis of two-dimensional nonlinear sloshing problems in random excitations," *Ocean Engineering*, 32, 107-133.

Wu, GX, Ma, QW, Taylor, RE (1998). "Numerical simulation of sloshing waves in a 3D tank based on a finite element method," *Applied Ocean Research*, 20 (6), 337-355.

Wu, CH, Chen, BF (2009). "Sloshing waves and resonance modes of fluid in a 3D tank by a time-independent finite difference method," *Ocean Engineering*, 36, 500-510.

Xue, MA, Lin, PZ (2011). "Numerical study of ring baffle effects on reducing violent liquid sloshing," *Computers & Fluids*, 52, 116-129.

Yang, YQ, Tang, ZY, Zhang, YL, Wan, DC (2015). "Investigation of Excitation Period Effects on 2D Liquid Sloshing by MPS Method," *Proceedings of the Twenty-fifth (2015) International Ocean Polar Engineering Conference*, Kona, Hawaii, USA, 3, 891-897.

Yang, YQ, Tang, ZY, Zhang, YL, Wan, DC (2015). "Numerical Simulation of 3D Sloshing Flows in a Rectangular Tank by MPS Method," *Proceedings of the 9th International Workshop on Ship and Marine Hydrodynamics*, Glasgow, UK.

Zhang, YX, Wan, DC (2012a). "Numerical Simulation of Liquid Sloshing in Low-Filling Tank by MPS," *Journal of Hydrodynamics*, 27, 100-107.

Zhang, YX, Wan, DC (2014). "Comparative study of MPS method and level-set method for sloshing flows," *Journal of Hydrodynamics*, 26 (4): 577-585.